FLUORINATED LANTHANIDE COMPLEXES:

NEW NIR-VIS UPCONVERSION SYSTEMS

BOGDANOV VIKTOR

SCHOOL OF PHYSICAL AND MATHEMATICAL SCIENCES

A thesis submitted to the Nanyang Technological University
in fulfilment of the requirement for the degree of
Master of Science

2017

Acknowledgements

First of all, I would like to express my deepest personal gratitude to my supervisor, Professor Xiong Qihua, for his caring and support throughout all my work, from the very beginning till the submission of the final thesis. His passion towards research in general bound with the great skill of seeing the grains of gold in the piles of dirty experimental data have made him an example of true expert of Nature in my eyes and to the great extent inspired my own work.

I also express special thanks to Dr. Huanqing Ye, who helped me master most of the experimental techniques employed in this work as well as ignited my interest in the particular research field. In fruitful discussions with him the scientific truth was forged and tempered, even sometimes for the price of our own temper.

Finally, I would like to appreciate the contribution of the rest of the group and the friends among the students and the faculty of NTU, without whom this work would have been finished much earlier but would have not been half as enjoyable.

Table of contents

Abstract

Lanthanide-based upconversion is a well-known process in solids, but for a wide variety of applications small size, preferentially molecular size upconversion emitters are required. Using inorganic upconversion nanoparticles solves some of the problems, however, the luminescence is severely quenched for smaller particle sizes. On the other hand, organic lanthanide complexes provide better overall luminosities and can be easily modified for medical applications, but rarely provide adequate quantum yield of NIR emission to enable upconversion processes.

This work was aimed to realize conventional for inorganic systems Yb-Tb/Er upconversion in the perfluorinated organic complex and study its mechanism in order to explore the limits of the system and evaluate the perspective pathway.

Green Yb-Tb upconversion by cooperative energy transfer (CET) mechanism was realized in vacuum, and green/red Yb-Er upconversion by energy transfer (ETU) mechanism was shown to be possible in ambient conditions for organic complex powder. Energy transfer pathways were studied in detail to explain features of the mechanisms, such as three-photon red upconversion for the latter case.

Based on this data the conclusion about the perspectives is drawn and the outlook of the future work in the field is provided.

1. Introduction

During the last century rare earth elements, most of which are lanthanides, were not only the matter of interest for scientists, but also gained an important role in our everyday life due to the variety of their newly emerged practical applications. In particular, these unique chemical elements became the essence of many advanced materials which are used in basically every piece of our common technology: electronics, optic communication, lighting, and display– all of them contain lanthanides in one or another form.[1]

All magnificent properties of lanthanides are due to their partially filled f-sublevel (4f) in electronic structure. f-orbitals in lanthanides are shielded by 5s and 5p electrons which make them chemically inactive and this explains very similar chemical properties of the whole row. The main difference between them is in the electronic configuration of 4f sublevel, which gives rise to the differences in energy spectra, and that is the reason why lanthanides attract so much attention.

Energy states of lanthanides possess several very important properties. First of all, due to the inner character of 4f orbitals, these energy states are virtually unaffected by the chemical environment of the ion, which makes energy spectrum a characteristic property of the lanthanide. Secondly, f-f transitions are partially forbidden due to the Laporte's parity selection rule in dipole approximation. From the practical viewpoint, it leads to long lifetimes of the excited states (in micro- and millisecond range) and low absorption and emission cross-sections. While the first one is the advantage which gives rise to the one of the most important properties of lanthanide-based systems – upconversion, the second one is a problem which is dealt with by introducing lanthanide ions into the proper organic matrix, forming lanthanide organic complexes.

Upconversion studies and lanthanide coordination chemistry are the two big fields with different advantages and challenges. For the efficient NIR to visible upconversion the basic requirement is a high quantum yield of lanthanide luminescence which is achieved by using inorganic crystals, nowadays mostly $NaYF_4$, as a host matrix.[2] In such systems one lanthanide element, usually Yb, is used as a sensitizer, which absorbs NIR light and transfers it to another lanthanide, called activator, which in its turn releases energy as visible irradiation. The major drawback of such systems is relatively low absorption cross-section of Yb^{3+} (compared to, for example, organic materials) which limits the overall luminosity, especially considering the typical doping concentrations of 2-5%.[2]

On the other hand, organic complexes work as an effective antenna for lanthanide ions, transferring energy from the ligand's triplet state to the lanthanide, thus, through the process of singlet ligand excitation – intersystem crossing – lanthanide sensitization, by several orders of magnitude increasing the overall luminosity of the system. Another advantage of organic complexes is the ability to engineer the organic surrounding via chemical synthesis to the suit the desired application.[3]

But the main problem in designing the efficient NIR-emitting organic complex is the vibrational quenching effect of the ligand due to the possibility of energy transfer from lanthanide excited state to the overtones of CH and OH vibrations with later non-radiative vibrational relaxation. Reasonably high luminescent quantum yields for Er^{3+} (~7%) and Yb^{3+} (~50%) were achieved for the fully fluorinated complex with N-{P,P-di(pentafluorophinoyl)}-P,P-dipentafluorophenylphosphinimidate (HF-TPIP, Fig. 1) as a ligand [4], [5], while other works, even that claim the synthesis of "highly luminescent" complexes, report the luminescent lifetimes of Yb^{3+} only of 10-20 μs which corresponds to <2% QY. [6], [7] Recently published research provides another perspective ligand for Yb^{3+} NIR emission, however, its structure is more complicated compared to

F-TPIP and the improvement in the internal quantum yield (63%) is achievable in the environment of hydrogen-free solvent, which is not seriously significant. [8]

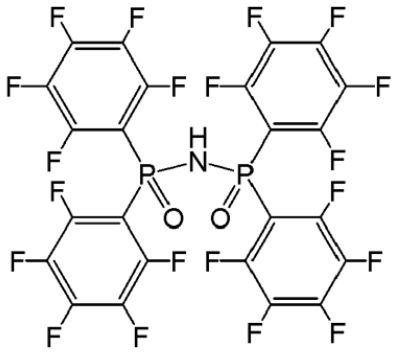

Fig. 1 *Structure of HF-TPIP*

Up to now there was virtually no connection between these two fields, despite the attempts to apply sensitization effect to solid state upconverters, namely upconversion nanoparticles (UCNP). In particular, there is a successful attempt to introduce dye-based sensitizer on the surface of the nanoparticles [9], but for the above stated reasons, there has never been reported an all-metalorganic upconversion system, potentially exploiting all the advantages of the coordination chemistry.

In this work the possibility of such systems is discussed, the evidence of upconversion processes in all-metallorganic material in solid state is presented, and the pathways of future work on the topic are considered.

2. Literature review

2.1 Intrinsic energy transitions in lanthanides

Energy transitions in lanthanide ions can be divided to two groups: interconfigurational $4f^n$-$4f^{n-1}5d^1$ and intraconfigurational f-f ones. Interconfigurational dipole transitions are parity allowed, but the typical energy of them lies in the $(30\text{-}80)\cdot10^3$ cm^{-1} range, which makes most of them typically non observable. [10]

Meanwhile the effect of ligand-field on the energies of spectroscopic levels is quite weak, for the f-f transitions its influence is determinant. In the absence of ligand-field dipole transitions between f-orbitals are parity forbidden, but the perturbation of the field leads to the parity mixing and, therefore, allowance of so-called induced electric dipole transitions. Mathematically this effect is usually treated by means of Judd-Ofelt theory. According to it, the dipole strength (in esu^2cm^2) of the induced transition between Ψ and Ψ' states is given by:

$$D_{ED} = e^2 \cdot \sum_{\lambda=2,4,6} \Omega_\lambda \cdot \left|\langle \Psi \| U^\lambda \| \Psi' \rangle\right|^2 \quad (1)$$

Where e is the electric charge of the electron, Ω_λ (in cm^2) are phenomenological Judd-Ofelt parameters obtained from the absorption spectrum, and U^λ are irreducible tensor forms of the ED operator. Bracketed values in this formula are tabulated matrix elements and independent of chemical environment of the ion. [11]

Apart from induced ED transitions, magnetic dipole (MD) and electric quadrupole (EQ) transitions are also allowed for the f-f transitions, but their strengths are 2 and 6 orders of magnitude less than induced ED ones, so in practice EQ transitions can be neglected. Dipole strengths of the MD transitions are given by:

$$D_{MD} = \left(\frac{e \cdot h}{4\pi \cdot m_e \cdot c}\right) \cdot \left|\langle \Psi \middle| L + 2S \middle| \Psi' \rangle\right|^2 \quad (2)$$

Selection rules for the above stated transitions, including the ones based on Judd-Ofelt theory, are listed in Tab. 1

Transition	**ΔS**	**|ΔL|**	**|ΔJ|**	**I_{rel}**
ED, 4f-5d	0	≤ 1	≤ 1	0.01-1
Induced ED, f-f	0	≤ 6 (2,4,6 if *L* or *L'* = 0)	≤ 6 (2,4,6 if *L* or *L'* = 0)	10^{-4}
MD, f-f	0	0	≤ 1	10^{-6}
EQ	0	≤ 2	≤ 2	10^{-10}

Tab. 1 Selection rules for lanthanide-based transitions [12]

Experimentally, the dipole strength (in esu^2cm^2) of the transition is calculated from the absorption spectrum using the formula [13]:

$$D_{exp} = \frac{3hc}{8\pi^3} \cdot \frac{1000 \cdot ln10}{N_A} \cdot \left((2J+1) \cdot \frac{9n}{(n^2+2)^2}\right) \cdot \int \frac{\varepsilon(\tilde{\nu})}{\tilde{\nu}} d\tilde{\nu} \quad (3)$$

Where $(2J + 1)$ represents the degeneracy of the initial state and the expression involving *n*, refractive index of the environment, is a Lorentz's local field correction for absorption.

Lanthanide absorption and emission happen accordingly to the above stated principles. Focusing on the lanthanide luminescence in particular, in the ideal case it happens as a spontaneous emission. Rate constant of such emission and the corresponding lifetime are conventionally called radiative. Quantitative description of the process can be obtained by considering Einstein's A coefficient, which represents the rate of spontaneous emission and is related to the dipole strength by the equation:

$$\frac{1}{\tau_{rad}} = k_{rad} = A = \frac{64\pi^4\tilde{\nu}^3}{3h(2J'+1)}D \tag{4}$$

Which, in case of theoretical evaluation of the radiative lifetime through D_{ED} and D_{MD}:

$$\frac{1}{\tau_{rad}} = k_{rad} = \frac{64\pi^4\tilde{\nu}^3}{3h(2J'+1)} \cdot \left(\frac{n(n^2+2)^2}{9}D_{ED} + n^3 D_{MD}\right) \tag{5}$$

And from the experimental data for absorption:

$$\frac{1}{\tau_{rad}} = k_{rad} = 8\pi c n^2 \tilde{\nu}^3 \cdot \frac{2J+1}{2J'+1} \cdot \frac{1000 \times ln10}{N_A} \cdot \int \frac{\varepsilon(\tilde{\nu})}{\tilde{\nu}} d\tilde{\nu} \tag{6}$$

In the presence of other, non-radiative decay processes, the observed decay rate would be:

$$k_{obs} = k_{rad} + \sum_i k_{nr}^i \tag{7}$$

Where k_{nr} represent non-radiative decay rates. Consequently, the quantum yield for the excited state, expressed through decay rates is:

$$Q = \frac{k_{rad}}{k_{obs}} = \frac{k_{rad}}{k_{rad} + \sum_i k_{nr}^i} = \frac{\tau_{obs}}{\tau_{rad}} \tag{8}$$

This quantum yield of the lanthanide emission under direct excitation is often called intrinsic and denoted as Q_{Ln}^{Ln}. [14] Therefore, experimental estimation of this quantity is available through time-resolved spectroscopy by measuring τ_{obs}, if the radiative lifetime is known.

2.2 Organic lanthanide complexes: sensitization and challenges

Since the f-f transitions of lanthanides, the ones which attract the most interest, are forbidden by symmetry, typical absorption coefficients are in the range 0.1-10 $M^{-1}cm^{-1}$[14], which is significantly lower than for organic luminophores with absorption coefficients ~10^4-10^5 $M^{-1}cm^{-1}$, which leads to poor overall luminosities ($L = \varepsilon \times Q$) of the materials under direct excitation of f-f transitions. However, in 1942 it was discovered, that ligand excitation of organic lanthanide complexes leads to the lanthanide excitation through the energy transfer and, hence, the emission from f-orbitals-based excited states. [15] The effect was called antenna effect for luminescence sensitization and gave rise to the broad field of lanthanide coordination chemistry.

The general pathway of luminescence sensitization of given on Fig. 2. The efficiency of this process is highly dependent on the relative energies of ligand's triplet state and lanthanide excited states. In particular for Eu emission from ^5D term the best result is achieved when triplet state of the ligand is 1200 cm^{-1} higher than $^5D_1$ level, while sensitization is sufficiently hampered for triplet states resonant to $^5D_0$ level due to back energy transfer and, finally disappears completely if the triplet level is lower than $^5D_0$. [16] Although to achieve full understanding of the sensitization process, roles of other states, namely ligand singlet state and ligand to metal charge transfer state, have to be considered, in this work we would not focus on it since for NIR-emitting lanthanides the biggest role in the overall quantum yield $Q_{Ln}^{L} = \eta_{sens} \times Q_{Ln}^{Ln}$ is played by the intrinsic quantum yield and not by sensitization efficiency.[14]

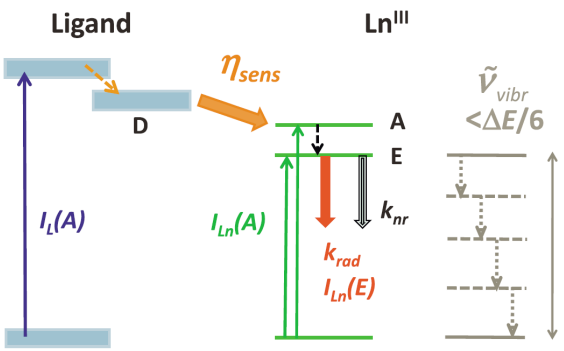

Fig. 2 *Luminescence sensitization scheme.* [14] $\boldsymbol{\eta_{sens}}$ *represents sensitization efficiency*

Considering various radiationless deactivation processes, the most important role among organic lanthanide complexes is played by vibrational quenching. This quenching occurs through energy transfer from lanthanide excited states to the phonons of different bound molecules and/or overtones of high-energy vibrations, namely CH and OH stretch vibrations. The involvement of phonons, consequently, leads to temperature dependence of such deactivation. [17] There is clear evidence, that non-radiative decay constants strongly depend on the energy gap of the transition: the quenching effect is significantly reduced when more than six phonons are required to fill the gap or the distance to the quencher is increased (Tab. 2). [18]

Ln	**ΔE_g, cm^{-1}**	**№ of phonons**		**k_{nr}^{OH}, s^{-1}**	**k_{nr}^{CH}, s^{-1}**	
		OH	**CH**	**2.2-2.5 Å**	**3.6-3.9 Å**	**5.0-5.3 Å**
Tb ($^5D_4$)	14800	4	5	100–200	12	–
Eu ($^5D_0$)	12200	3-4	4	400-500	40	–
Yb ($^4F_{5/2}$)	10300	3	3-4	3.5×10^5	3.6×10^4	1.7×10^3
Dy ($^4F_{9/2}$)	7850	2-3	3	2×10^4	9×10^3	4.3×10^3
Sm ($^4G_{5/2}$)	7400	2	2-3	1.8×10^4	9×10^3	6.0×10^3
Er ($^4I_{11/2}$)	6600	2	2	$(3\text{-}5)\times10^8$	–	3.3×10^6

Tab. 2 *Luminescence quenching by high-energy vibrations* [19]

From the theoretical viewpoint, considering Förster's mechanism (through dipole-dipole interaction) of non-radiative decay [20], the rate constant of the process can be expressed as [21]:

$$k_{nr} = \frac{9k_r\kappa^2}{128\pi^2 n^4 r^6} \cdot \frac{1000 \cdot ln10}{N_A} \cdot \int \frac{I_{norm}(\tilde{\nu}) \cdot \varepsilon_{vib}(\tilde{\nu})}{\tilde{\nu}^4} d\tilde{\nu} \qquad (9)$$

Where r is the distance between lanthanide and quencher, κ is a factor depending on relative orientations of f-f and vibrational transition dipole moments, n is the refractive index of the medium, I_{norm} is the emission spectrum normalized per unit area and ε_{vib} is the vibration absorption coefficient. However, obtaining the data for such calculation is challenging, even though the reported results are well consistent with the experiment.[21]

According to the above stated, eliminating the vibrational quenching is conceptually simple and can be illustrated by the data from [22], summed up in Tab. 3 and Fig. 3

Complex·solvate	**τ, ms**	**Q, %**
$Yb(DBM\text{-}H)_3 \cdot 2H_2O$	1	0.023
$Yb(DBM\text{-}H)_3 \cdot DMSO\text{-}d_6$	17.4	0.73
$Yb(DBM\text{-}D)_3 \cdot DMSO\text{-}d_6$	30.1	1.26
$Yb(TTA\text{-}H)_3 \cdot DMSO\text{-}d_6$	27.3	2.16
$Yb(TTA\text{-}D)_3 \cdot DMSO\text{-}d_6$	71.8	6.1

Tab. 3 *Lifetimes and QY of different Yb complexes* [22]

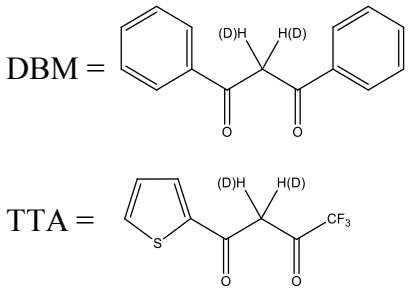

Fig. 3 *Structures and abbreviations of ligands used in* [22]

According to this work, replacement of coordinated solvent with the one without OH or CH bonds increases the lifetime for at least an order of magnitude, further replacement of close CH bonds ($\tilde{\nu}_{CH} \approx$ 2800-3000 cm^{-1}) with CD ones ($\tilde{\nu}_{CD} \approx$ 2100-2200 cm^{-1}) increases the lifetime another two times, while replacement of one of the moieties with the CF_3 group ($\tilde{\nu}_{CD} \approx$ 2100-2200 cm^{-1}) leads to one of the best reported results. Therefore, usage of halogenated ligands, that preferably prevent solvent coordination is crucial for the effective NIR emission.

2.3 Upconversion processes

Upconversion – converting of low-energy photons, e.g. IR ones, to high-energy, namely in visible and UV regions – is a well-known process in lanthanide co-doped solids, acknowledged at least in the 1960's. [23] Nowadays the scope of upconversion studies switched from the bulk solids, useful for purely optical applications, like lasers, to nanoparticles – the ones, receiving a significant interest due to their applications in mostly bioimaging, but not narrowed down to it. [24] From the fundamental viewpoint, looking deep into the origins of the process, several mechanisms of lanthanide upconversion are known and, therefore, discussed in this chapter.

2.3.1 Energy transfer upconversion (ETU)

This mechanism is, by far, the most effective and the most studied one among all. Schematic representation of such process is given in Fig. 4. There are two lanthanide ions involved in the process: sensitizer, which absorbs IR light, and activator, emitting light in visible range. The crucial parameter, required for this mechanism, is the presence of the intermediate state of the activator. Thus, in a typical ETU process, the first step is usually direct sensitizer excitation. Yb^{3+} is most commonly used as a sensitizer due to its relatively large (in comparison to other lanthanides) absorption cross-section and the simplicity of the spectrum. [25] Then the intermediate state of the activator is populated both by direct laser excitation and non-radiative energy transfer from sensitizer. From the intermediate state, excitation to the higher emissive state occurs by dipole-dipole resonant energy transfer from the sensitizer – therefore the name of the process.

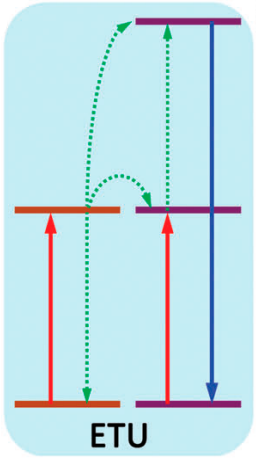

Fig. 4 *Schematic representation of ETU mechanism* [26]

Since the crucial requirement is the presence of intermediate states, and considering Yb as the most common sensitizer, only several lanthanides, the ones with energy levels somewhat resonant with $^2F_{5/2}$ level of Yb, are suitable for such a process. Usually only there are used as activators in nanoparticles – Ho^{3+}, Er^{3+} (for green/red emission) and Tm^{3+} (for blue/UV emission).

For the upconversion process to occur, significant lifetime of the excited states of sensitizer and activator is essential. Therefore, the majority of works consider UC processes in various kinds of solids, due to the absence of vibrational quenching by OH and CH bonds. Instead the factors, that contribute most to the quenching are defects (in bulk crystals) [25] and surface effects (in nanoparticles) [26]. Also, an important role in luminescence quenching in solids is played by inter-ion energy transfer processes between sensitizers/activators. Such energy hopping from one ion to another leads to bigger probability of non-radiative deexcitation and, consequently, luminescence quenching, therefore, doping concentrations for inorganic materials are usually kept low. [26]

Despite the overwhelming number of works dealing with inorganic upconversion systems, there surprisingly exist some dealing with upconversion processes in organic-based matrices. The article [27] can be used to illustrate the possibility of ETU upconversion process in the organic complex, where Er ion is sandwiched between two Cr^{3+} ones. Cr ions are used as sensitizers for UC luminescence, absorbing light close to the edge of visible spectrum, at 750 nm. Then typical Er emission with wavelengths of 540-560 nm occurs. The emission is possible due to the mechanical protection of Er ion from surrounding quenchers. It is significant to note, that, according to this work, the UC intensity is significantly better in solution than in solid state, presumably due to strong inter-ion quenching effect of sensitizers.

Another interesting work about Er^{3+} ETU upconversion is [28], where UC process is observed in a 2-center complex, linked by F^- ion. Without any other lanthanides, Er serves both as sensitizer and activator for itself. Therefore, close proximity of Er ions plays the major role in the process. Upconversion unit is, again, shielding Er ion from CH and OH quenchers – which is also essential.

2.3.2 Excited state absorption (ESA)

This upconversion mechanism is much less efficient, than ETU one, but in many cases, they behave similar. As evident from the scheme on Fig. 5, the lanthanide subjected to ESA should also have an intermediate state. The difference is that, in contrast with ETU mechanism, this process is single-centered and, therefore, doesn't require any sensitizer, either external, or of the same kind, which makes it possible to occur with very low concentrations. However, the requirements for this process are large absorption cross-section for both ground and excited states (which is absolutely uncommon in lanthanides), and, obviously, long lifetime of the excited state – which is impossible to achieve for high doping concentrations for the above discussed reasons. As a result, in practice this process is observed only in Er-doped systems, where for one reason or another ETU process is not available. [25]

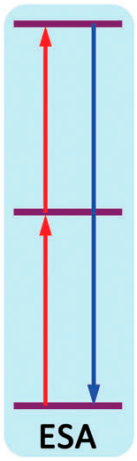

Fig. 5 *Schematic representation of ESA mechanism* [26]

2.3.3 Cooperative energy transfer (CET)

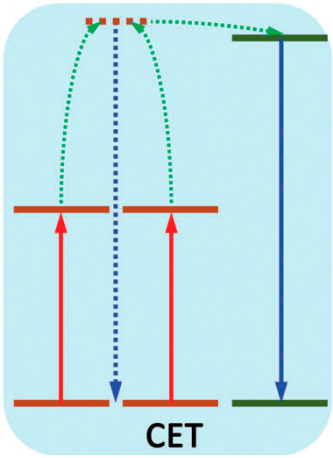

Fig. 6 *Schematic representation of CET mechanism* [26]

This mechanism, depicted in Fig. 6, usually occurs when activators are absent of intermediate states, resonant with the excited state of the sensitizer (Yb^{3+}). According to this mechanism, energy transfer to the activator happens from the virtual cooperative state of two sensitizers. Activators, that are suitable for such process, should bear the emissive state close to the two times of sensitizer gap frequency. Any energy mismatch leads to the requirement of photon assistance for bridging two gaps, which reduces the total efficiency of the process. [29] Therefore, from the practical viewpoint, only Tb^{3+} and Eu^{3+} show CET upconversion – or at least their UC processes are the most widely studied.

While in most cases CET upconversion is shown for the lanthanide-doped inorganic substances [30], [31], there is one particular work where the possibility of lanthanide upconversion in polymer system was investigated. [29] In it, authors showed, that embedding lanthanide pairs, namely Yb/Er and Yb/Tb, into perfluorinated polymer matrix (using perfluorobutanesulfonate as a ligand) leads to a bright red and green UC respectively. Interesting observation, that deviate this work from the ones performed on inorganic systems, is the unusual power dependence of UC emission.

In most cases, upconversion intensity is proportional to the radiation power to the power of n ($I_{UC} \propto P^n$), where n represents the number of photons, involved in the process. [32] For green and red UC emission when excitation is to the $^2F_{5/2}$ level of Yb^{3+} it gives $n = 2$ for any mechanism. [30], [33], [34], while $n = 3$ in the similar conditions for blue UC emission.[35] In the case of organic matrix, however, n turned out to be 4.7 for green light and 6.9 for red light. [29] Such effect was attributed to laser heating with respective

increase of Yb^{3+} absorption cross-section [36] – and laser heating is not something unusual in organic systems with an abundant vibrational modes.

To sum up, upconversion processes have received a great attention since the very first discovery. Different mechanisms of the process have been investigated and accepted for lanthanide-doped inorganic materials. However, only a few UC studies have been done on organic-based system due to the presence of vibrational quenching which significantly limits the UC efficiency. In particular, there is no known attempts to design the conventional UC system with Yb^{3+} as a sensitizer, and the limits of the field are yet to explore.

2.4 HF-TPIP – ultimate ligand for NIR emission

As it was previously discussed, obtaining NIR emission from lanthanide ions in organic complexes is a challenging task, that demands the development of the ligand which will be as absent of high energy vibrations as possible and at the same time would prevent coordination of the solvent. Luckily, the synthesis of such a ligand - N-{P,P-di(pentafluorophinoyl)}-P,P-dipentafluorophenylphosphinimide (HF-TPIP) was reported [37] together with the increase of the Er^{3+} IR luminescence ($^4I_{15/2}$-$^4I_{13/2}$ transition) lifetime from previous record of several microseconds to at least 224 μs as a major (92%) component of biexponential decay in thermal evaporated film.

More detailed study on F-TPIP complexes of lanthanides were presented two years later, together with Nd^{3+} and Yb^{3+} IR luminescent lifetimes (44 μs and 1111μs in CD_3CN solutions respectively), and also even better Er^{3+} one (741 μs in CD_3CN solution). [5] Apart from spectral analysis on those complexes, this work also gave a hindsight on the reason of such outstanding result. Crystal structures of the complexes have been obtained, and, according to them, there is indeed no solvent coordinated to NIR-emitting lanthanides. Fig. 7 represents crystal structure of $Yb(F\text{-}TPIP)_3$.

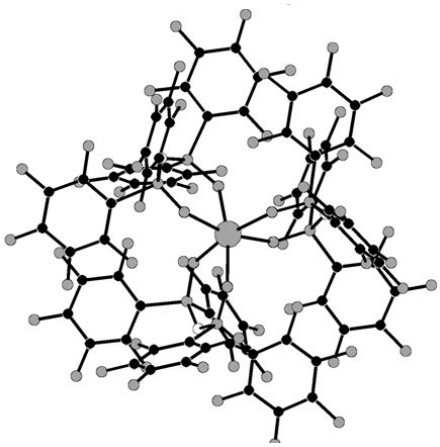

Fig. 7 *Crystal structure of* $Yb(F\text{-}TPIP)_3$ [5]

The advancements didn't pass unnoticed, and later on two works were published by H.Q. Ye et.al. [38][4], with both of them featuring $Er(F\text{-}\ TPIP)_3$. The first one dealt with thoughtful analysis of fundamental effects of fluorination on the radiative properties of Er^{3+}. In this work Judd-Ofelt parameters for a variety of Er^{3+} complexes, including $Er(F\text{-}\ TPIP)_3$ were determined and the results were compared to the experimentally determined line strength. According to these results, radiative lifetime of $^4I_{15/2}$ state in $Er(F\text{-}\ TPIP)_3$ is 12.6 ms [38], and this parameter is a crucial etalon for luminescence efficiency determination.

The other work was more applied, where authors reported a smart design of a waveguide and an IR OLED, based on mixed $Zn(F\text{-}BTZ)_2/Er(F\text{-}\ TPIP)_3$ system. Er luminescence lifetime in such conditions was showed to be 860 μs which gives ~7% intrinsic QY – by far, the highest reported result. More important, this result was obtained in solid state, which is more than 2 times bigger than previous one in the similar conditions for this complex. [5] With such result for NIR-emitting ions, the development of an upconversion system is a logical step forward.

3. Experimental details

3.1 Equipment and methods

3.1.1 VIS/NIR spectroscopy

Absorption spectra in solutions were registered using Perkin-Elmer Lamda 950 UV/Vis/NIR spectrometer.

Photoluminescence spectra, including upconversion fluorescence ones, were registered using home-made system which consists an iHR320 (Horiba Scientific) spectrometer equipped with 1200 and 600 lines/mm gratings and detected using photomultiplier tubes 1911FPMT (Horiba Scientific) for the 190 – 860 nm wavelength region and H10330B NIR-PMT (Hamamatsu) for the infrared (920 – 1700 nm) region. Luminescence data was extracted using an SR830 DSP lock-in amplifier (Stanford Research Systems) with the SR540 optical chopper (Stanford Research Systems) on the optical path providing a reference frequency. All emission spectra were corrected for the spectrometer response.

975 nm diode laser (MDL-III-975R-500mW, CNI Optoelectronics Tech. Co.) was used as the light source for photoluminescence and upconversion photoluminescence measurements. The light was focused on the sample using either the lens system or 50X infinity corrected objective (Mitutoyo Plan Apo NIR) yielding a minimum available spot of 0.2 mm^2 which corresponds to ~110 W/cm^2 power density. For power-dependent measurements laser power was measured using Newport 843-R power meter equipped with 919P series detector.

3.1.2 Time-resolved measurements

The light source for nanosecond pulse pumped photoluminescence experiments was an Optical Parametric Oscillator (MagicPrism^{TM}, OPOTEK) laser pumped by a Q-

Switched Nd:YAG (Quantel's BrilliantB-20Hz). The duration of laser pulse is ~ 5 ns. For the upconversion-related time-resolved measurements, an above mentioned 975 nm diode laser (MDL-III-975R-500mW, CNI Optoelectronics Tech. Co.) was modulated with a TTL signal from a pulse generator (TT*i*, TGP110, 10MHz) to give long (~40 ms) pulses with a rise/decay time of < 30 μs. Time-resolved photoluminescence traces were extracted from a 300MHz oscilloscope (Aglient InfiniiVision 6000 series). The traces were fitted using exponential functions with $R^2 > 0.998$.

3.1.3 NMR spectroscopy

$^{19}F\{^1H\}$ and $^{31}P\{^1H\}$ NMR spectra were recorded using Bruker AV300 spectrometer. Acetone-d_6 was used as a solvent for all registered spectra. Orthophosphoric acid was used as an external reference for ^{31}P shifts, and $C_6H_5CF_3$ was the internal reference for ^{19}F shifts.

3.2 Materials synthesis and characterization

White HF-TPIP acid powder (200 mg, 0.26 mmol, > 98% Changzhou Jiade Pharmtech Co. Ltd, China was dissolved in boiling solvent mixture (1:1 volume ratio) of ethanol (absolute, analytical grade, Fischer Scientific) and methanol (HPLC/ACS grade, Anhui Fulltime Specialized Solvent & Reagent Co., Ltd). 0.09 mmol of lanthanide salts mixture ($YbCl_3$ (anhydrous, 99.998% trace metals basis, Sigma-Aldrich Ltd.), YCl_3 . (anhydrous, 99.99% trace metals basis, Sigma-Aldrich Ltd.), $ErCl_3$ (anhydrous, 99.99% trace metals basis, Sigma-Aldrich Ltd.) or $TbCl_3$ (anhydrous, 99.99% trace metals basis, Sigma-Aldrich Ltd.)) with the desired lanthanides ratio was weighted, dissolved in 2 ml of the same mixture of solvents and added to the stirring solution of HF-TPIP. The solution was heated under reflux for 20 minutes and allowed to cool to room temperature. White precipitate was then separated using a centrifuge and washed with the ethanol/methanol solvent mixture to remove the unreacted starting materials. The precipitate was then dried under 70℃ for over 10 hours. Some portions of the powders were purified by vacuum

sublimation at 10^{-6} mbar pressure and the temperature between 250℃ to 300℃. Typical yield is 80-98%.

Yb(F-TPIP)$_3$: $^{31}P\{^1H\}$ NMR (121 MHz, [D_6]acetone): δ = –1.2 (s) $^{19}F\{^1H\}$ NMR (282MHz, [D_6]acetone): δ = –136.0 (d, ^3J(F,F)=18 Hz, 24F, *o*-ArCF), –149.0 (t, ^3J(F,F)=19 Hz, 12F, *p*-ArCF), –163.4 (br, 24F, *m*-ArCF);

Tb(F-TPIP)$_3$: $^{31}P\{^1H\}$ NMR (121 MHz, [D_6]acetone): δ = –24.1 (br) $^{19}F\{^1H\}$ NMR (282MHz, [D_6]acetone): δ = –134.0 (br, 24F, *o*-ArCF), –150.8 (br, 12F, *p*-ArCF), –164.4 (br, 24F, *m*-ArCF);

Er(F-TPIP)$_3$: $^{31}P\{^1H\}$ NMR (121 MHz, [D_6]acetone): δ = –47.0 (s) $^{19}F\{^1H\}$ NMR (282MHz, [D_6]acetone): δ = –134.5 (br, 24F, *o*-ArCF), –149.5 (br, 12F, *p*-ArCF), –163.4 (br, 24F, *m*-ArCF);

Y(F-TPIP)$_3$: $^{19}F\{^1H\}$ NMR (282MHz, [D_6]acetone): δ = –135.1 (d, ^3J(F,F)=20 Hz, 24F, *o*-ArCF), –149.9 (t, ^3J(F,F)=18 Hz, 12F, *p*-ArCF), –163.7 (br, 24F, *m*-ArCF);

This result mostly agrees with the literature data for various Ln(F-TPIP)3 complexes. [5] ~13 ppm difference in ^{31}P shift for Tb(F-TPIP)$_3$ can be attributed to the differences in solvent coordination to lanthanide which is known to happen for Tb(F-TPIP)$_3$. [5]

For all of the complexes the signal of *p*-ArCF can be used as an analytical signal for confirming the ratio between lanthanide complexes in mixed materials. The ratio of the signals was found to be consistent (±10 %) with the ratio of the lanthanide chlorides used in the synthesis thus confirming the proportions of the lanthanide ions in the studied materials.

4. Results and discussion

4.1 Yb – Tb upconversion luminescence

All results, discussed in this subchapter, was obtained in collaboration with Huanqing Ye, a postdoctoral fellow in the group of Prof. Xiong Qihua, who played a leading role in experimental work, while I participated by material synthesis and characterization, discussions, while simultaneously learning experimental techniques. The results, presented in other subchapters of the section, are experimentally obtained by myself and thoroughly discussed with the above-mentioned persons.

The advancement in NIR luminescence of lanthanides in complexes gave rise to the particular interest in the ability to obtain effective Yb^{3+} luminescence. To acquire a radiative lifetime, absorption measurement of $Yb(F\text{-}TPIP)_3$ in $DMSO{:}CH_3CN$ 1:1 was performed (Fig. 8) and the parameter was estimated from the formula (6). $\tau_{rad} = 1.1 \pm 0.1\, ms$, which is consistent with literature, where the radiative lifetime of Yb^{3+} $^2F_{5/2}$ in complexes is in the range 0.7 – 2.0 ms. [39]

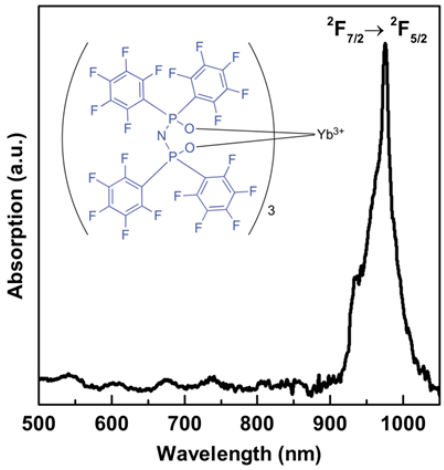

Fig. 8 *Absorption spectrum of $Yb(F\text{-}TPIP)_3$ in $DMSO{:}CH_3CN$ 1:1*

Experimental evaluation of Yb^{3+} $^2F_{5/2}$ excited state lifetime was performed on $Yb_xY_{1-x}(F\text{-}TPIP)_3$ mixed complexes in two forms: powder purified by vacuum sublimation, and thermally evaporated 200 nm thin film. Y^{3+}, being optically transparent in NIR region, is conventionally used as dilutant to achieve desired lanthanide ion density. Air pressure was varied to eliminate moisture, absorbed by the material. The results are given in Fig. 9.

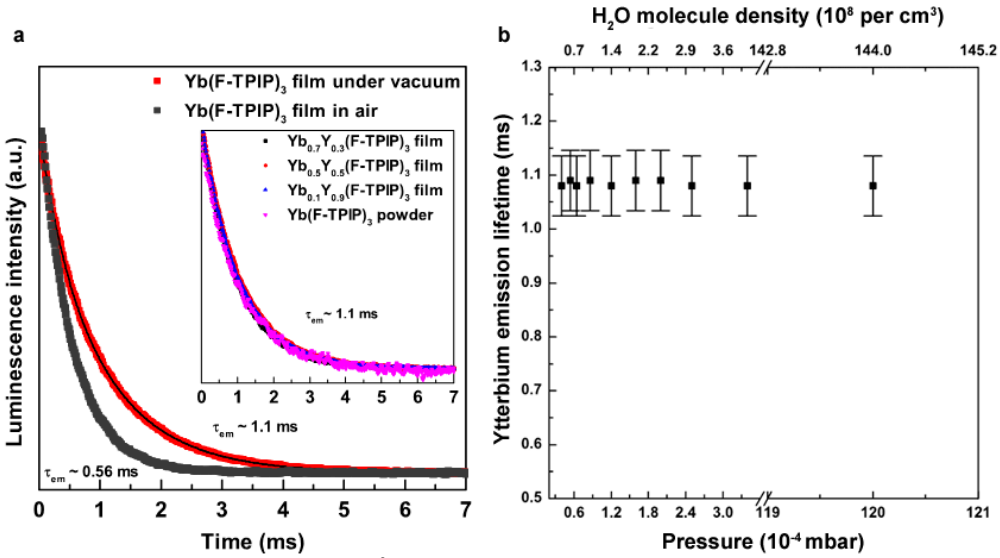

Fig. 9 *(a) 1050 nm emission ($^2F_{7/2}$ line) decay curves in various complexes and various conditions. (b) Vacuum dependence of 1050 nm emission lifetimes in $Yb_{0.7}Y_{0.3}(F\text{-}TPIP)_3$*

The lifetime of Yb^{3+} $^2F_{5/2}$ in ambient conditions (0.56 ms) is consistent with the literature data for $Yb(F\text{-}TPIP)_3$ emission lifetime in powder form (0.58 ms). [5] However, putting the sample in vacuum significantly increases this parameter, pushing it up to the the theoretical limit of 1.1 ms, which gives $Q_{Ln}^{Ln} \approx 100\%$. The most probable reason for such behaviour is vacuum desorption of moisture, that resuces the amoint of quenchers in the material. The lifetime in vacuum is then independent of the form (powder or thin film), part of Yb^{3+} in $Yb_xY_{1-x}(F\text{-}\ TPIP)_3$ mixed complex (from 0.1 to 1), and the exact level of vacuun (from $1.2\cdot10^{-2}$ to $0.6\cdot10^{-4}$ mbar). The result is also independent of the purification level of the material: Yb^{3+} lifetime in non-purified by vacuum sublimation $Yb(F\text{-}TPIP)_3$ turned out to be the same.

To test the upconversion properties, mixed complex $Yb_{0.7}Tb_{0.3}(F\text{-}TPIP)_3$ was synthesized. Tb in this system has been chosen as an activator due to radiative character of its $^5D_4$ level: once it is excited, all transitions are radiative in visible region, in contrast with Er^{3+}, where deactivation processes can non-radiatively occur to $^4I_{13/2}$ level on which the

role of vibrationcal quenching is significantly higher. The proportion between Yb^{3+} and Tb^{3+} is chosed according to [29] to maximize upconversion intensity.

Expected Yb-Tb bright green upconversion was indeed observed in the material, placed in 10^{-2} mbar vacuum. (Fig. 10) Unusual power dependende of the Tb emission, previously reported for co-doped fluorinated polymers, [29] indicate the presence of laser heating of the sample.

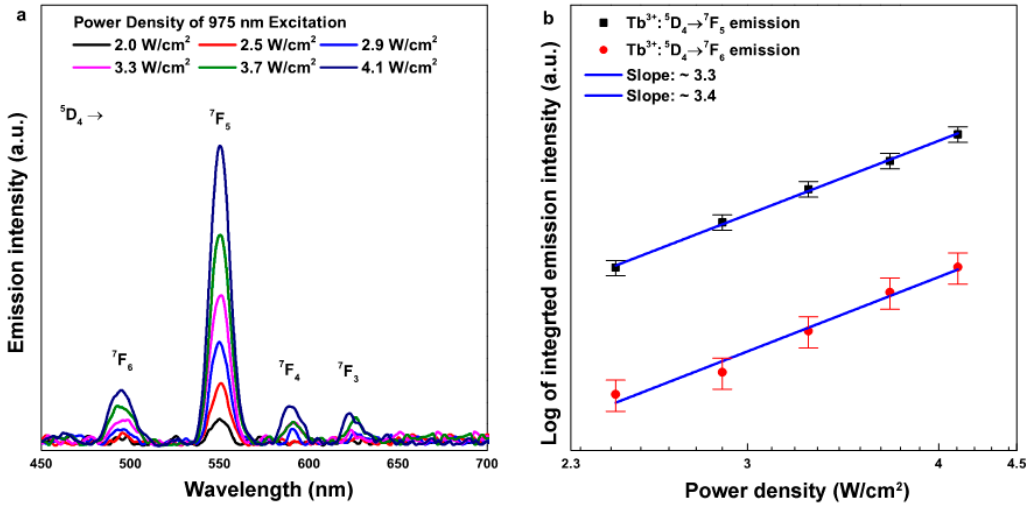

Fig. 10 *(a) UC emission intensity of* $Yb_{0.7}Tb_{0.3}(F\text{-}TPIP)_3$ *in* 10^{-2} *mbar vacuum at 975 nm excitation. (b) Power dependence of Tb upconversion emission line intensities*

More interesting effect appears upon placing the material in the higher vacuum, 10^{-5} mbar. Even brighter, red upconversion emission appears and easily overcomes Tb emission. (Fig. 11)

The spectrum doesn't show any characteristic features in visible region and was assumed to be blackbody radiation spectrum. Planck's law fitting of spectra converges with R2 > 0.999, which supports the assumption. Interestingly, in the NIR region Yb^{3+} luminescence is much more intense than blackbody radiation, however, careful consideration of the NIR region shows the same expected thermal radiation pattern together with the presence of trace amounts of Er impurities.

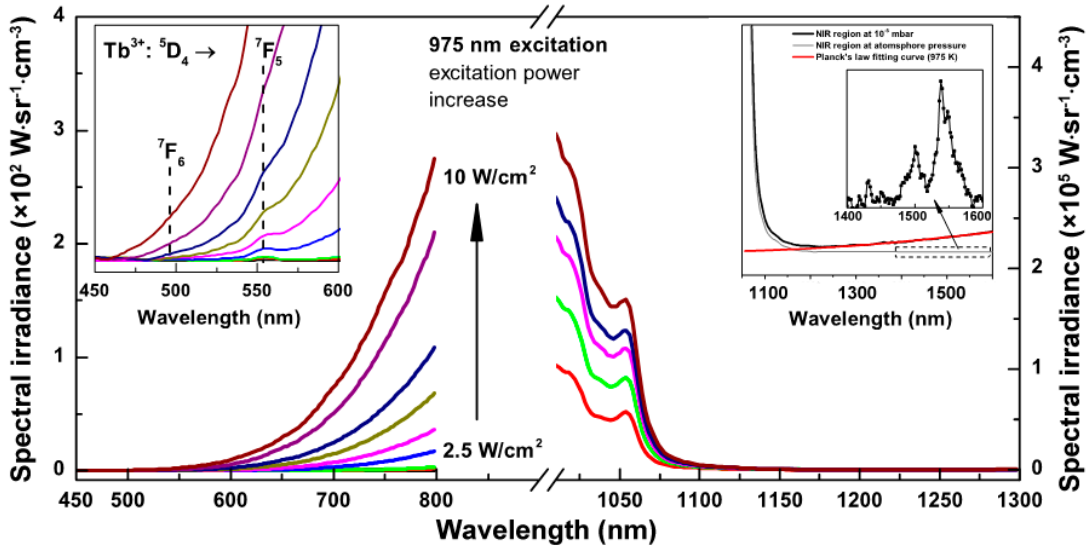

Fig. 11 *UC emission intensity of $Yb_{0.7}Tb_{0.3}(F\text{-}TPIP)_3$ in 10^{-5} mbar vacuum at 975 nm excitation. The visible region (450 to 800 nm) primarily exhibits the visible fraction of the thermal radiation with the Tb emission peaks (Tb^{3+} $^5D_4 \rightarrow {}^7F_{6,5}$) buried (zoom in, left inset). The NIR region (1010 to 1300 nm) primarily exhibits the ytterbium emission. Magnified NIR region in different pressure conditions is plotted with in the right inset together with Planck's law fitting.*

To explore the limits and estimate the role of Tb in blackbody radiation upconversion, power dependence measurements were performed on $Yb_{0.7}Tb_{0.3}(F\text{-}TPIP)_3$ and $Yb_{0.7}Y_{0.3}(F\text{-}TPIP)_3$. Emission spectra were registered and fitted with the Planck's law, yielding blackbody temperatures, plotted in Fig. 12. According to it, presence of Tb^{3+} reduces the power threshold, required for thermal UC to occur. Maximum blackbody temperature was found to be approximately 1300 K, after reaching which the material turned out to decompose with respective loss is UC efficiency.

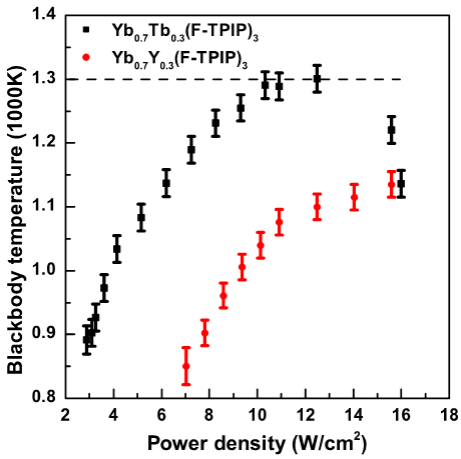

Fig. 12 *Planck's law estimated blackbody temperatures of $Yb_{0.7}Tb_{0.3}(F\text{-}TPIP)_3$ and $Yb_{0.7}Y_{0.3}(F\text{-}TPIP)_3$*

Enegry transfer pathways were further clarified by time-dependence measurements. Yb^{3+} and Tb^{3+} were directly excited by 5ns pulse laser to their respective spectroscopic levels ($^2F_{5/2}$, 975 nm and $^5D_4$, 487 nm) to determine their lifetimes (Fig. 13a), and for the same in UC process 38 ms square pulse 975 nm laser excitation was employed (Fig. 13b and Fig. 13a inset).

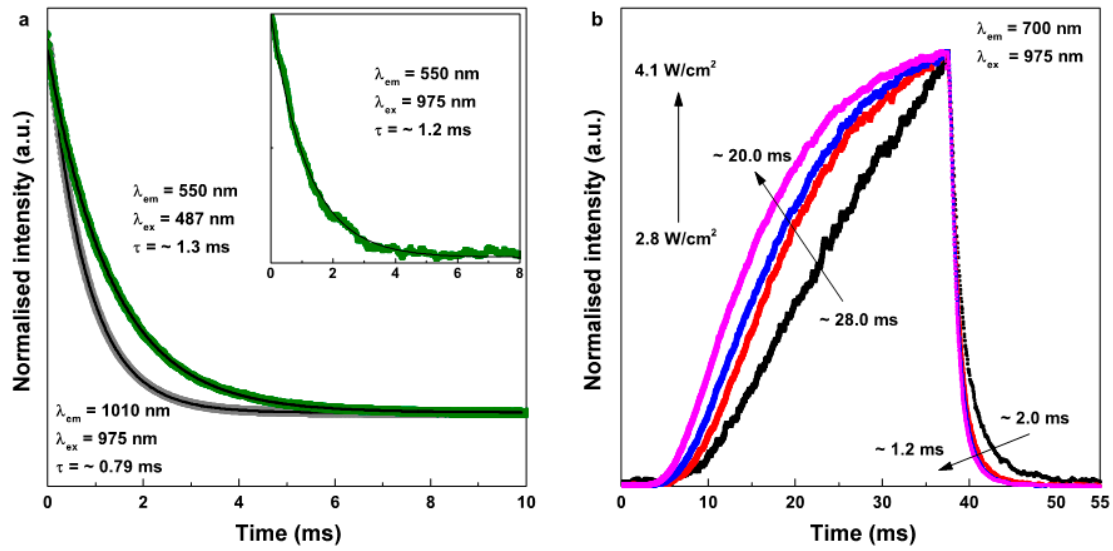

Fig. 13 *(a) Ytterbium emission (grey dots) for 975 nm excitation using a 5.0 ns pulse; Tb^{3+}:$^5D_4$-$^7F_5$ emission (green dots) when directly excited to $^5D_4$ level using a 5 ns pulse at 487 nm excitation; Tb^{3+}:$^5D_4$-$^7F_5$ emission (green dots, the inset) when excited using a square 38.0 ms pulse at 975 nm excitation; Fitting curves (black lines) are using single exponential functions. (b) UC through thermal radiation recorded at 700 nm wavelength when excited using a square 38.0 ms pulse at 975 nm excitation with varied excitation power*

In $Yb_{0.7}Tb_{0.3}$(F-TPIP)$_3$ system the lifetime of Yb^{3+} is quenched to ~ 0.79 ms which indicates the presence of energy transfer, which is not surprising considering the presence of Yb-Tb UC process in the system. From this data the rate of the Yb-Tb enerty transfer rate can be estimated $k_{Yb-Tb} = (\tau_{Yb}^{UC})^{-1} - (\tau_{Yb}^{rad})^{-1} \approx 340\ s^{-1}$, which is slightly more efficient than in Yb-Tb doped polymer [29]. Tb^{3+} emission lifetime in UC is not significantly different from the luminescent one, which means that the role of $^5D_4$ state in thermal UC is negligible. However, this lifetime is lower than the one reported for Tb in this complex is solution, which might indicate the concentration quench of Tb^{3+} luminescence.

Thermal UC emission on 700 nm features a build up time, which redues with the increase of laser. Interestingly, the rise time is ~ 10 times longer than the decay time over the explored excitation power. This difference could be due to the presence of thermal convection between the high-temperature $Tb(F\text{-}TPIP)_3$ and the low-temperature $Yb(F\text{-}TPIP)_3$, hence longer time is needed to build up the heat due to the thermal dissipation.

Combining everything about this case, the phenomenon can be explained as follows: Yb^{3+} gets excited to its $^2F_{5/2}$ level by incident irradiation at 975 nm, then energy is transferred to $^5D_4$ level of Tb^{3+} by CET upconversion mechanism. Both radiative and non-radiative energy transfer from this level populate lower $^7F_{3\text{-}5}$ levels of Tb^{3+}. These levels have relative energy in 2000-4000 cm^{-1} range and, therefore, undergo vibrtional relaxation, transferring energy to F-TPIP ligand, where the vibrational modes span the range from 600 to 1650 cm^{-1}. This mechanism in schematically illustrated by Fig. 14.

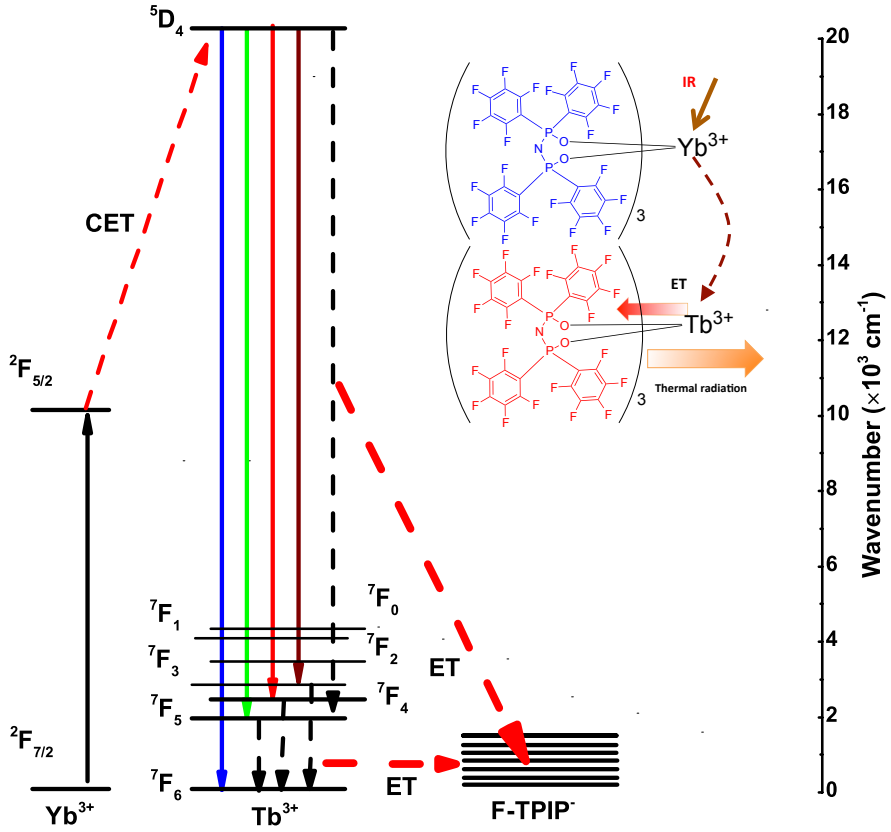

Fig. 14 *Mechanism of upconversion processes in* $Yb_{0.7}Tb_{0.3}(F\text{-}TPIP)_3$

4.2 Yb – Er upconversion luminescence

Upconversion by ETU mechanism is known to be much more efficient, than by CET [2], however, for it to occur non-radiative processes should be minimized for both sensitizer and activator, which is a challenging task since lowest energy levels for all common activators, such as erbium ions, lie lower, than $^2F_{5/2}$ level of Yb^{3+}.

4.2.1 Er^{3+} $^4I_{13/2}$ lifetimes in ambient conditions

The lifetime of the lowest excited state of the ion limits the energy transfer efficiency and, therefore, ultimately influences upconversion. [2] Hence, determination of the emission lifetime and its dependency from the concentration of the ion in the material is a relevant starting point.

For Yb^{3+} emission the work is already discussed in the previous subchapter, showing the absence of concentration quench in $Yb_xY_{1-x}(F\text{-}TPIP)_3$ for x in range from 0.1 to 1. In ambient conditions Yb^{3+} $^2F_{5/2}$ emission, excited by 975 nm 4 ns laser pulse, exhibits biexponential decay with average lifetime $\tau_{Yb}^0 = 560 \pm 20\,\mu s$, or, in terms of rate constants $k_{Yb}^0 = 1/\tau_{Yb}^0 = (1.8 \pm 0.1) \cdot 10^3\ s^{-1}$ which corresponds to the internal quantum yield of $Q_{Yb}^{Yb} = \tau_{Yb}^0/\tau_{Yb}^{rad} \approx 50\%$.

The same idea was employed to investigate the concentration quench of Er^{3+} $^4I_{13/2}$ emission. A set of $Er_xY_{1-x}(F\text{-}TPIP)_3$ complexes was prepared, excited by 975 nm 4 ns laser pulse, and the time-resolved 1540 nm emission traces were registered for each one. Single-exponentially fitted lifetime data is presented in Fig. 15.

According to this data, concentration quench in the complex is inconspicuous on the detectable level regardless the concentration of the Er^{3+} ion. The lifetime of $^4I_{13/2}$ level $\tau_{Er}^0 = 120 \pm 10\,\mu s$, which in terms of rate constants is $k_{Er}^0 = (8.3 \pm 0.7) \cdot 10^3\ s^{-1}$ and corresponds to the internal quantum yield of $Q_{Er}^{Er} \approx 1\%$ taking $\tau_{Er}^{rad} = 12\ ms$. [38]

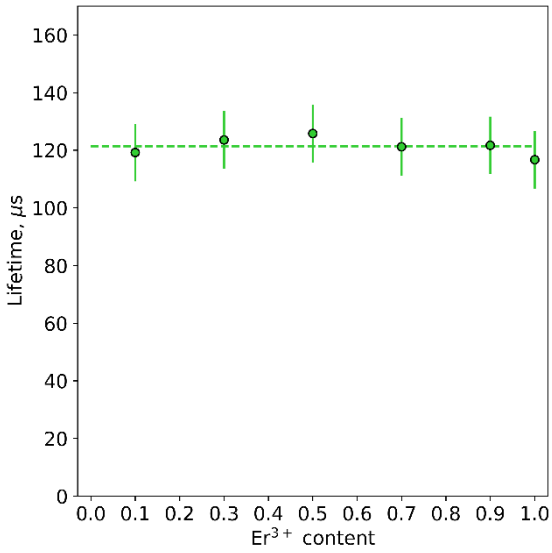

Fig. 15 *Er^{3+} $^4I_{13/2}$ lifetimes in Er_xY_{1-x}(F-TPIP)$_3$*

4.2.2 Yb^{3+} to Er^{3+} energy transfer

High quantum yield of Yb^{3+} emission due to the reduced quenching effect of the environment facilitates useful non-radiative energy transfer such as Yb-sensitized upconversion. For earlier discussed $Yb_{0.7}Tb_{0.3}$(F-TPIP)$_3$ complex Yb^{3+} to Tb^{3+} energy transfer constant was estimated to be $k_{Yb-Tb} = \left(\tau_{Yb}^{with\ Tb}\right)^{-1} - \left(\tau_{Yb}^{rad}\right)^{-1} \approx 340\ s^{-1}$, which means that in atmosphere this process (and, hence, upconversion) is overwhelmed by the quenching with effective constant $k_{quench} = (\tau_{Yb}^{atm})^{-1} - \left(\tau_{Yb}^{rad}\right)^{-1} \approx 900\ s^{-1}$.

In contrast with unresonant Yb^{3+} to Tb^{3+} CET process, close energies of Yb^{3+} $^2F_{5/2}$ and Er^{3+} $^4I_{11/2}$ levels conventionally give rise to the resonant energy transfer process and, consequently Yb^{3+} to Er^{3+} energy transfer upconversion (ETU).

Since ETU upconversion occurs mostly due to the interaction between Yb^{3+} $^2F_{5/2}$ and Er^{3+} $^4I_{11/2}$ excited stated, with, in the best case, both of them pumped simultaneously by the same light source, theoretically the most efficient molar ratio of the ions should be 1:1. Thus, $Yb_{0.5}Er_{0.5}$(F-TPIP)$_3$ complex was synthesized and for the purpose of energy transfer investigation time-resolved emission from Yb^{3+} $^2F_{5/2}$ (1050 nm) and Er^{3+} $^4I_{13/2}$ (1540 nm) levels was registered under 975 nm 4 ns laser pulse excitation (Fig. 16).

This picture clearly indicates the presence of the significant energy transfer process: lifetime of $Yb^{3+}\ {}^2F_{5/2}$ is reduced to 160 μs, giving effective Yb^{3+} to Er^{3+} energy transfer constant $k_{Yb-Er} \approx 4500\ s^{-1}$ - bigger, than quenching constant for $Yb^{3+}\ {}^2F_{5/2}$ in atmosphere.

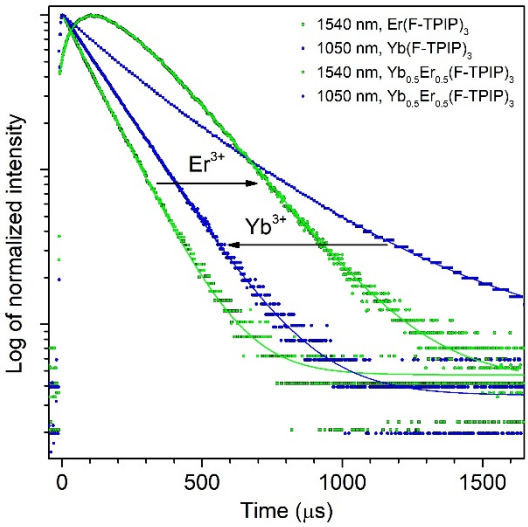

Fig. 16 *$Er^{3+}\ {}^4I_{13/2}$ and $Yb^{3+}\ {}^2F_{5/2}$ emission traces in $Er(F\text{-}TPIP)_3$, $Yb(F\text{-}TPIP)_3$ and $Er_{0.5}Yb_{0.5}(F\text{-}TPIP)_3$. Solid lines represent single- (for two bottom traces) and double- (for two top ones) exponential fittings.*

The trace of $Er^{3+}\ {}^4I_{13/2}$, on the other hand, indicates the competition of excitation and deexcitation processes, with rate constants of $k_{Er-rise} \approx 9000\ s^{-1}$ and $k_{Er-decay} \approx 5300\ s^{-1}$ accordingly derived from the biexponential fitting of the trace. $k_{Er-rise}$ is bigger than k_{Yb-Er},which indicates the presence of the $Er^{3+}\ {}^4I_{13/2}$ pumping process apart from $Yb^{3+}\ {}^2F_{5/2} \rightarrow Er^{3+}\ {}^4I_{11/2} \rightarrow Er^{3+}\ {}^4I_{13/2}$ energy transfer. However, only the presence of such process cannot explain the reduced decay constant of $Er^{3+}\ {}^4I_{13/2}$ in comparison to non-Yb^{3+}-containing sample. To gain insight on the nature of energy transfer processes in the material, two sets of samples, containing Y^{3+} as dilutant were prepared. In the first set, $Yb_xEr_{0.5}Y_{0.5-x}(F\text{-}TPIP)_3$, Er^{3+} share was fixed to 0.5 therefore, making Er^{3+} concentration in the material constant.

Fig. 17 and Tab. 4 show no significant difference in $Yb^{3+}\ {}^2F_{5/2}$ emission from the Yb^{3+} concentration, which was expected, taking into account previously shown absence of concentration quench in the material. Variation of Yb^{3+} concentration also shows no effect on the rate constants of $Er^{3+}\ {}^4I_{13/2}$ emission.

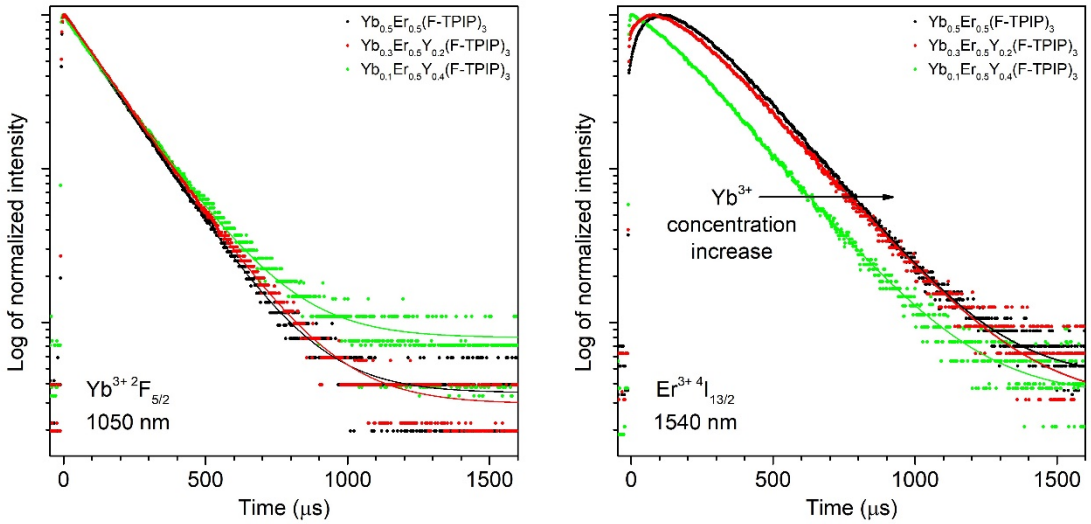

Fig. 17 *Yb^{3+} $^2F_{5/2}$ (left) and Er^{3+} $^4I_{13/2}$ (right) emission traces in $Yb_xEr_{0.5}Y_{0.5-x}$(F-TPIP)$_3$. Solid lines represent single- (for Yb^{3+} $^2F_{5/2}$ luminescence and Er^{3+} $^4I_{13/2}$ luminescence in $Yb_{0.1}Er_{0.5}Y_{0.4}$(F-TPIP)$_3$) and double- (for other Er^{3+} $^4I_{13/2}$ luminescence) exponential fittings.*

Yb^{3+} content	**Rate constant, $\cdot 10^3$ s^{-1}**		
	1050 nm	**1540 nm**	
	Decay	**Decay**	**Rise**
0.1	6.0	5.0	–
0.3	6.1	5.2	9.2
0.5	6.3	5.3	9.1

Tab. 4 *Rate constants for* ***Fig. 17***

In the second set of samples, $Yb_{0.5}Er_xY_{0.5-x}$(F-TPIP)$_3$, Yb^{3+} share was fixed to 0.5 and Er^{3+} share was varied. The results of time-resolved PL measurements are presented in Fig. 18 and Tab. 5.

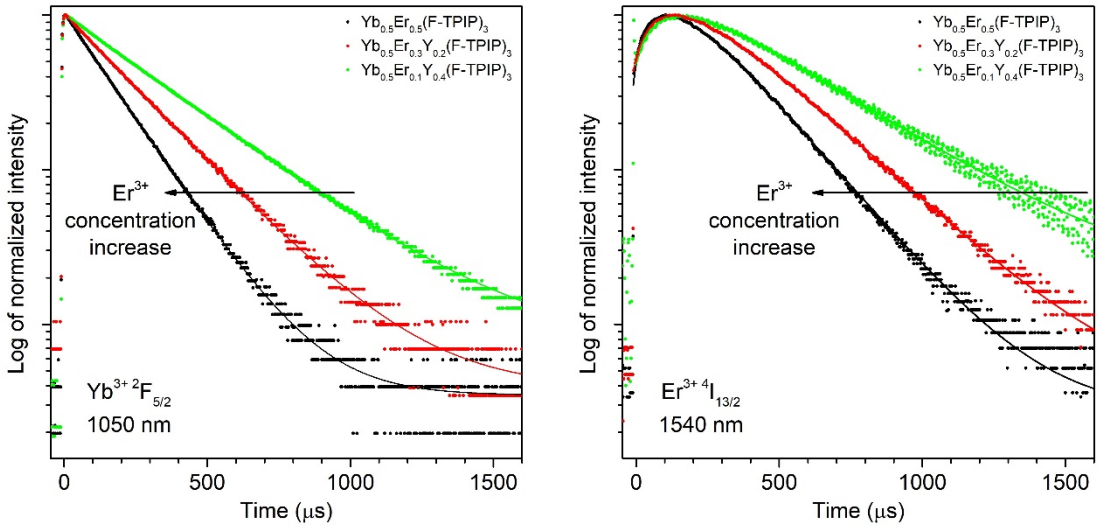

Fig. 18 *$Yb^{3+}\ ^2F_{5/2}$ (left) and $Er^{3+}\ ^4I_{13/2}$ (right) emission traces in $Yb_{0.5}Er_xY_{0.5-x}(F\text{-}TPIP)_3$. Solid lines represent single- (for $Yb^{3+}\ ^2F_{5/2}$ luminescence) and double- (for $Er^{3+}\ ^4I_{13/2}$ luminescence) exponential fittings.*

Er^{3+} content	Rate constant, $\cdot 10^3\ s^{-1}$		
	1050 nm	1540 nm	
	Decay	Decay	Rise
0.1	3.1	2.7	8.3
0.3	4.4	3.9	8.2
0.5	6.3	5.3	9.1

Tab. 5 *Rate constants for Fig. 18*

With the increase of Er^{3+} concentration in the material both $Yb^{3+}\ ^2F_{5/2}$ and $Er^{3+}\ ^4I_{13/2}$ decay constants increase. For $Yb^{3+}\ ^2F_{5/2}$ the data for both sample sets is consistent with the presence of $Yb^{3+}\ ^2F_{5/2} \rightarrow Er^{3+}\ ^4I_{11/2}$ energy transfer. Together with the invariance of $Yb^{3+}\ ^2F_{5/2}$ lifetime from Yb^{3+} concentration we can conclude the negligible role of all $Yb^{3+}\ ^2F_{5/2}$ population processes but absorption in the material under nanosecond pulse excitation. In particular, we can rule out $Er^{3+}\ ^4I_{11/2} \rightarrow Yb^{3+}\ ^2F_{5/2}$ back energy transfer. The absence of

such energy transfer is also supported by the downconversion studies: excitation of all of the above-mentioned materials to the Er^{3+} $^4F_{7/2}$ level by 488 nm 4 ns laser pulse produces negligible luminescence at 1050 nm and the lifetime of Er^{3+} $^4I_{13/2}$ luminescence in all cases lies within the error of τ_{Er}^0 - the lifetime of Er^{3+} $^4I_{13/2}$ in the absence of Yb^{3+}.

The dependence of Er^{3+} $^4I_{13/2}$ decay constants on Er^{3+} concentration in the material is also explainable by the presence of Yb^{3+} $^2F_{5/2} \rightarrow Er^{3+}$ $^4I_{11/2}$ energy transfer. Decay rate constant for this level in two-exponential treatment is lower, than k_{Er}^0, which implies, that the limiting stage is not the decay from the $^4I_{13/2}$ level itself, but the population of this level. The scheme of the relevant processes in the proposed mechanism is presented in Fig. 19. All of the processes have been previously reported for different Yb/Er systems, mostly inorganic lanthanide-doped nanoparticles. [2]

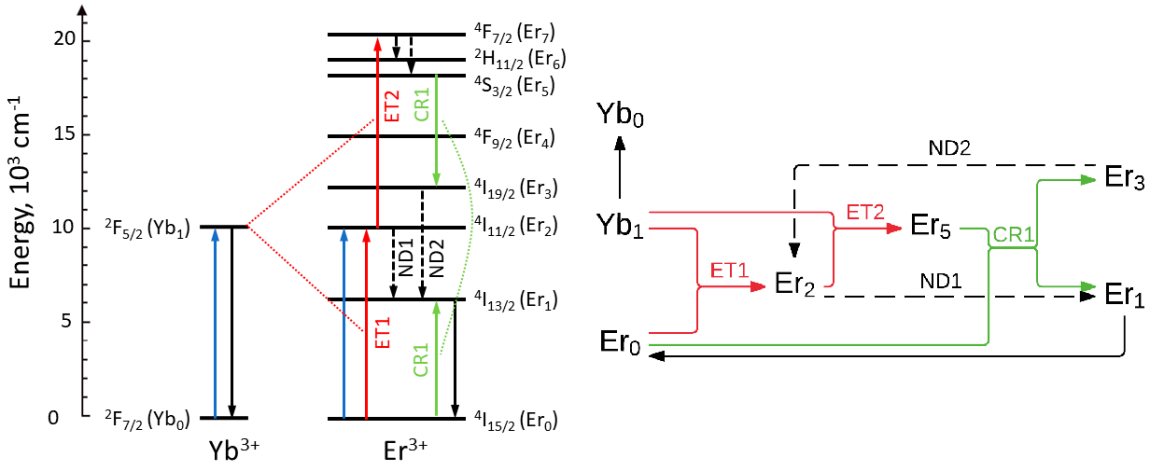

Fig. 19 *Some of the processes, characteristic for the system, and their kinetic scheme. Energy transfers (ET) are highlighted in red, cross-relaxations (CR) are green and non-radiative decays are dashed. Blue is absorption and black is effective decay with* $\boldsymbol{k_{Er}^0}$ *or* $\boldsymbol{k_{Yb}^0}$*, both radiative and non-radiative.*

In the absence of Yb^{3+} in the system the kinetic scheme of $^4I_{13/2}$ (Er_1) is simply:

$$Er_2 \xrightarrow{k_{ND1}} Er_1 \xrightarrow{k_{Er}^0} Er_0$$

Where Er_2 level is populated by direct absorption and $k_{ND1} > k_{Er}^0$, therefore, the decay with the rate of k_{Er}^0 is observed.

In the presence of Yb^{3+}, however, repopulation of Er2 level by ET1 process exists, and in case of $k_{ND1} > k_{Er}^0 > k_{ET1}$ will limit the rate of luminescence, which is observed in the experiment.

In all of the processes due to the low absorption coefficients of lanthanides the population of the excited states is negligible in comparison with the amount of ions in the ground state, therefore, the concentration of Er_0 in the material can be treated as constant equal to the concentration of Er^{3+} ions. Thus, all second-order processes involving erbium ground state can be treated as quasi-first-order ones with the rate constant linearly depending on the Er^{3+} concentration (or, considering roughly the same density of all F-TPIP complexes, Er^{3+} content).

Therefore, if ET1 is the dominating deexcitation process for Yb_1, and sumiltaneously dominating process of generation Er_1, limiting its decay, then both Yb_1-Yb_0 (1050 nm) and Er_1-Er_0 (1540 nm) luminescence should exhibit linear dependence on the Er^{3+} content. However, it has to be noticed, that the slope of such dependence might not be the same for the luminescences due to the presence of cross-relaxation processes which also depend on the Er^{3+} content, and rigorous quantitative analysis of the energy transfer kinetics is hampered by the complexity of the system.

Experimental data for content-dependent luminescence (Fig. 20) agrees with the mechanism described above. Both 1050 nm and 1540 nm luminescence exhibit linear dependence on Er^{3+} content with the intercepts on the limits of it equal to the k_{Yb}^0 and k_{Er}^0 within the experimental error.

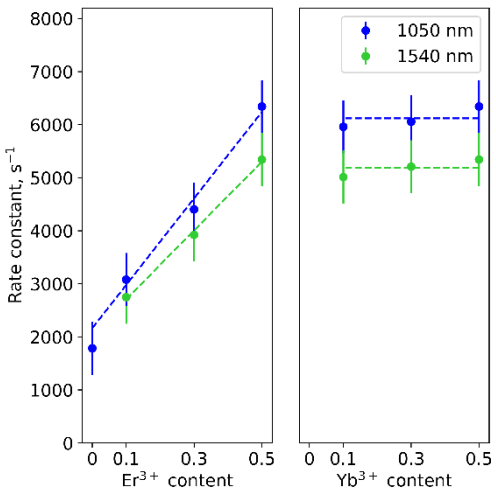

Fig. 20 *Dependence of luminescence rate constants from lanthanide content*

Thus, several important conclusions can be drawn from this time-resolved analysis:

- Population of lowest Er^{3+} excited states at any time is limited by the energy transfer from the $^2F_{5/2}$ level of Yb^{3+}, which, in turn is limited by Er^{3+} content. Therefore, for the purpose of upconversion Er^{3+} content should be kept low.
- Due to the high decay rate constant from the $^4I_{13/2}$ level the role of it in the UC process is expected to be negligible.
- No effect on the energy transfer was observed by variation of Yb^{3+} content, therefore, to increase the overall luminosity it can be maximised without compromising the UC efficiency.

4.2.3 Upconversion by ETU mechanism

For the reasons described in the previous subsection, $Yb_{0.9}Er_{0.1}(F\text{-}TPIP)_3$ was chosen as the material of primary investigation. Upconversion in green (515-575 nm) and red (640-685 nm) regions was observed for the material (Fig. 21).

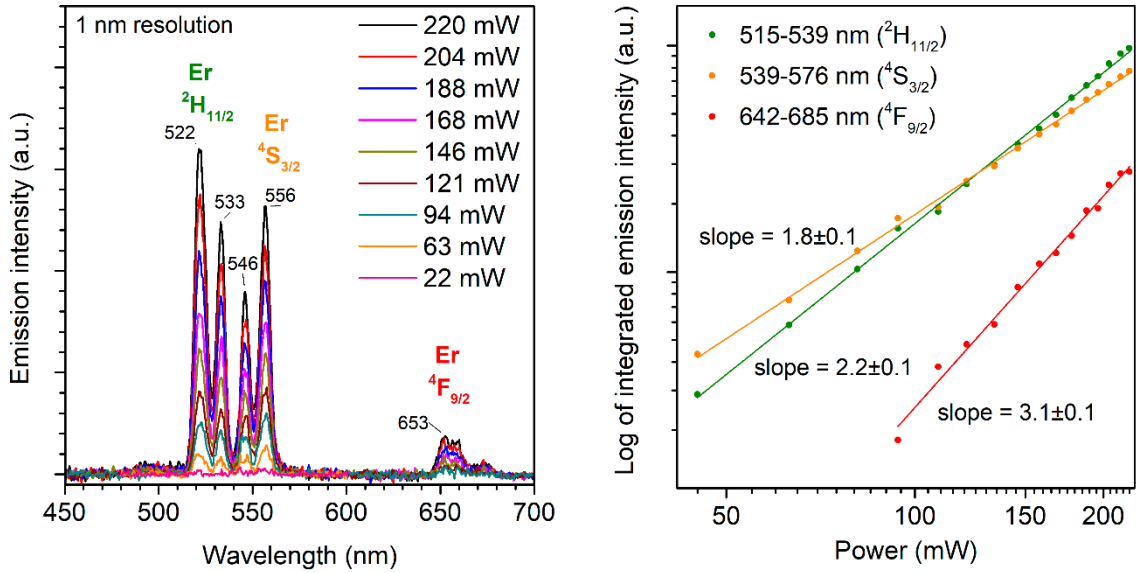

Fig. 21 *Upconversion spectra and power dependence for* $Yb_{0.9}Er_{0.1}(F\text{-}TPIP)_3$

Green upconversion luminescence from $^2H_{11/2}$ and $^4S_{3/2}$ levels behaves as a two-photon process, which is generally accepted due to the nature of the level population by the ET2 process (refer to Fig. 19). [2]

Red upconversion from the $^4F_{9/2}$ level, on the other hand, exhibits unusual 3-photon character. The same pattern in power-dependent luminescence is also observed in the $Yb_{0.7}Er_{0.3}(F\text{-}TPIP)_3$ and $Yb_{0.5}Er_{0.5}(F\text{-}TPIP)_3$ complexes (Fig. 22), but with the lower UC emission intensity, which makes it characteristic for the material.

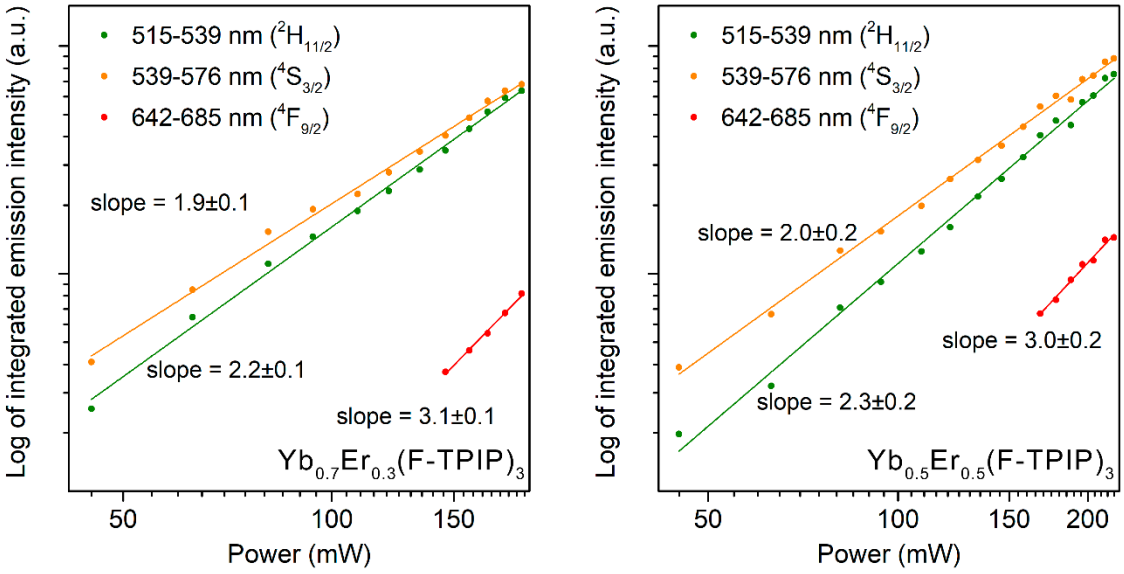

Fig. 22 *Power dependence of UC luminescence for $Yb_{0.7}Er_{0.3}(F\text{-}TPIP)_3$ and $Yb_{0.5}Er_{0.5}(F\text{-}TPIP)_3$*

Usual 2-photon mechanism of red upconversion is described by ETU process from the $^4I_{13/2}$ level of Er^{3+} [2], [40], [41], and 3-photon mechanism was observed in some works for Yb/Er doped β-$NaYF_4$ at high laser powers and explained as change in dominant process of $^4I_{13/2}$ population from ND1 (1-photon) to CR1 (2-photon) [2] (Fig. 19). Here, however, due to the low lifetime of the $^4I_{13/2}$ level 3-photon red upconversion have to be described by a different process, and we suggest another CR process (CR2), involving $^2H_{11/2}$ and $^4I_{11/2}$ levels instead since such process was also previously reported for Er-doped Y_2O_3. [42]

Overall, based on the experimental data, described in this section and section 4.2.2 and comparison to the literature, main processes responsible for the upconversion in the material are suggested in Fig. 23.

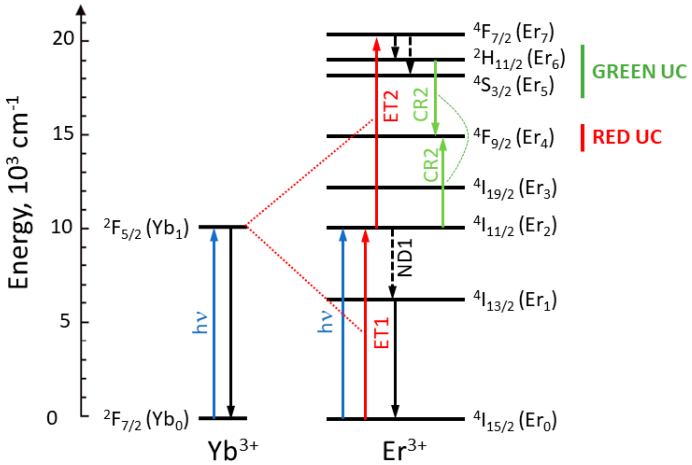

Fig. 23 *Suggested energy transfer processes responsible for the upconversion in $Yb_xEr_y(F\text{-}TPIP)_3$*

5. Further plans

5.1 Lanthanide variation

Both upconversion mechanisms, CET and ETU, were shown to be operational in F-TPIP based lanthanide materials. Moreover, Yb – Er upconversion has been achieved even in ambient conditions. These results inspire further research in this area and exploring the limits. In particular, two other lanthanides are interesting to try: holmium and thulium. The first one usually gives red UC emission, while the second one is capable of blue and even UV emission. [2] These three lanthanides, combined together, might be employed in NIR-white light upconversion, and organic matrix make these materials versatile for many potential applications.

5.2 Chemical modification of HF-TPIP

In an attempt to modify the ligand, nucleophilic substitution of para-fluorine by an azide group was proposed and tried, yielding HF-TPIP-N_3, even though details are leaved beyond the scope of this thesis. Such modification opens the way to further functionally modify the ligand in two ways. The first one is Cu^I-catalyzed "click" reaction with substituted alkyne to afford substituted 1,2,3-triazole ring [43] according to the scheme:

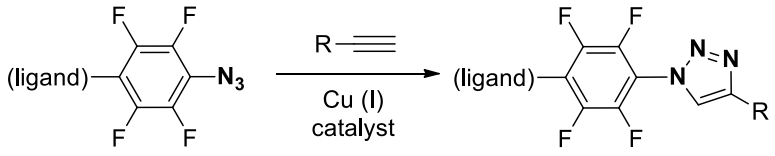

Enhanced solubility

The choice of R is, in fact, limited only by the availability of the corresponding alkyne. For example, it's reasonable to try modifying the ligand this way with R = C_6H_5, since phenylacetylene is a simple and commercially available compound.

The other way is to obtain an azo-ligand, which is slightly more elaborate, two-stage process. The overall scheme of the process is:

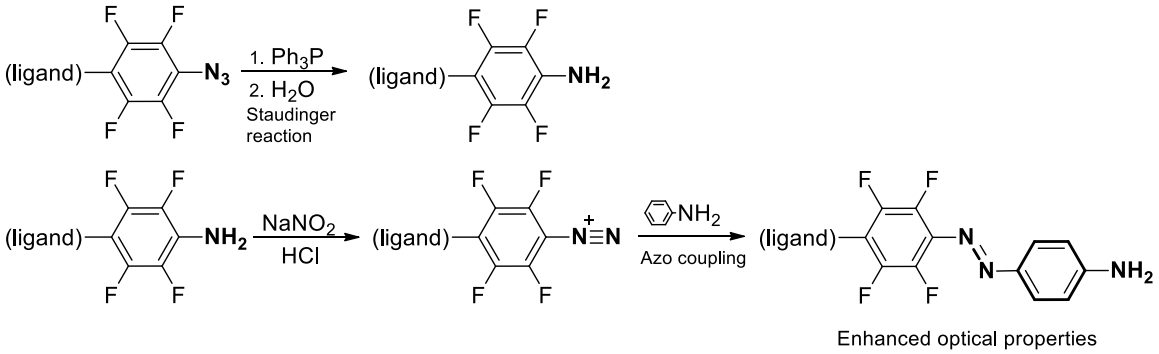

The first step of the process is $N_3 – NH_2$ conversion of the azide group known as Staudinger reaction. [44] The second step is known as azo-coupling and conventionally used in dye synthesis. [45] Practically this reaction includes *in situ* generation of diazonium ion by sodium nitrite oxidation followed by the azo-coupling with aromatic amine. The tunability of the reaction is provided by the choice of this amine. The simplest amine that can be used in this reaction to produce conjugated p-electron system is aniline (phenylamine). Therefore, due to the commercial availability of the aniline, it remains the primary target for such modification.

6. Conclusion

Lanthanide-based materials are being actively used in a variety of high-technological applications, and the demand of those applications fuel the intense search for new materials. Lanthanide organic complexes and upconversion nanoparticles are one of the most popular fields with their own challenges. Nowadays there is a little connection between them, even though several works have been published considering UC processes in organic complexes.

In this work, we have shown the possibility of UC processes in the organic-based material via two different mechanisms – CET and ETU – and explained the features of these mechanisms in detail. Remarkably, bright green Yb – Er upconversion by ETU mechanism has been observed in air, which inspire further research in this area designing new UC systems with various activators and experimentally probing these systems in the most perspective applications.

Together with Yb – Tb CET upconversion, another phenomenon – thermal upconversion – has been observed in this material at high vacuum. Thermal UC has been shown to be more intense than Tb^{3+} emission at the same power density, which makes it perspective to the certain extent.

The way to overcome drawbacks such as low solubility and high singlet state energy of HF-TPIP based materials has been proposed and justified. The first experimental step in such chemical synthesis has been probed, yielding regioselectively modified HF-TPIP-N_3 with azide groups substituting all 4 *para*-fluorines, as designed. Thus, the basis for further research has been provided.

7. Bibliography

[1] J.-C. G. Bünzli and S. V. Eliseeva, "Lanthanide NIR luminescence for telecommunications, bioanalyses and solar energy conversion," *J. Rare Earths*, vol. 28, no. 6, pp. 824–842, 2010.

[2] H. Dong, L.-D. Sun, and C.-H. Yan, "Energy transfer in lanthanide upconversion studies for extended optical applications," *Chem. Soc. Rev.*, vol. 44, no. 6, pp. 1608–1634, 2015.

[3] L. Armelao *et al.*, "Design of luminescent lanthanide complexes: From molecules to highly efficient photo-emitting materials," *Coord. Chem. Rev.*, vol. 254, no. 5–6, pp. 487–505, 2010.

[4] H. Q. Ye *et al.*, "Organo-erbium systems for optical amplification at telecommunications wavelengths.," *Nat. Mater.*, vol. 13, no. 4, pp. 382–6, 2014.

[5] P. B. Glover *et al.*, "Fully fluorinated imidodiphosphinate shells for visible- and NIR-emitting lanthanides: Hitherto unexpected effects of sensitizer fluorination on lanthanide emission properties," *Chem. - A Eur. J.*, vol. 13, pp. 6308–6320, 2007.

[6] Z. Zhang *et al.*, "PMMA-supported hybrid materials doped with highly near-infrared (NIR) luminescent neutral trikis-β-diketonate Yb3+ complex," *Inorg. Chem. Commun.*, vol. 52, pp. 53–55, 2015.

[7] T. Zhang *et al.*, "Water-soluble mitochondria-specific ytterbium complex with impressive NIR emission," *J. Am. Chem. Soc.*, vol. 133, no. 50, pp. 20120–20122, 2011.

[8] J.-Y. Hu *et al.*, "Highly near-IR emissive ytterbium(iii) complexes with unprecedented quantum yields," *Chem. Sci.*, vol. 8, no. 4, pp. 2702–2709, 2017.

[9] W. Zou, C. Visser, J. a. Maduro, M. S. Pshenichnikov, and J. C. Hummelen, “Broadband dye-sensitized upconversion of near-infrared light,” *Nat. Photonics*, vol. 6, no. 8, pp. 560–564, 2012.

[10] P. Dorenbos, “The 4fn- 4fn- 15d transitions of the trivalent lanthanides in halogenides and chalcogenides,” *J. Lumin.*, vol. 91, no. 1, pp. 91–106, 2000.

[11] J. L. Prather, “Atomic energy levels in crystals,” 1961.

[12] P. A. Tanner, “Some misconceptions concerning the electronic spectra of tri-positive europium and cerium,” *Chem. Soc. Rev.*, vol. 42, no. 12, pp. 5090–5101, 2013.

[13] C. Gorller-Walrand and K. Binnemans, “Spectral intensities of f-f transitions,” in *Handbook on the Physics and Chemistry of Rare Earths vo. 25*, K. A. Gschneidner Jr and L. Eyring, Eds. Amsterdam: Elsevier Science B.V., 1998.

[14] J.-C. G. Bünzli, “On the design of highly luminescent lanthanide complexes,” *Coord. Chem. Rev.*, vol. 293–294, pp. 19–47, 2015.

[15] S. I. Weissman, “Intramolecular energy transfer the fluorescence of complexes of europium,” *J. Chem. Phys.*, vol. 10, no. 4, pp. 214–217, 1942.

[16] S. Sato and M. Wada, “Relations between intramolecular energy transfer efficiencies and triplet state energies in rare earth $β$-diketone chelates,” *Bull. Chem. Soc. Jpn.*, vol. 43, no. 7, pp. 1955–1962, 1970.

[17] Y. Haas and G. Stein, “Pathways of Radiative and Radiationless Transitions in Europium(III) Solutions: the Role of High Energy Vibrations,” *J. Phys. Chem.*, vol. 75, no. 24, pp. 3677–3681, 1971.

[18] V. L. Ermolaev and E. B. Sveshnikova, “The application of luminescence-kinetic methods in the study of the formation of lanthanide ion complexes in solution,” *Russ.*

Chem. Rev., vol. 63, no. 11, pp. 905–922, 1994.

[19] V. L. Ermolaev and E. B. Sveshnikova, "The application of luminescence-kinetic methods in the study of the formation of lanthanide ion complexes in solution," *Russ. Chem. Rev.*, vol. 63, no. 11, pp. 905–922, 1994.

[20] I. M. Clarkson, R. S. Dickins, A. S. de Sousa, and others, "Non-radiative deactivation of the excited states of europium, terbium and ytterbium complexes by proximate energy-matched OH, NH and CH oscillators: an improved luminescence method for establishing solution hydration states," *J. Chem. Soc. Perkin Trans. 2*, no. 3, pp. 493–504, 1999.

[21] C. Doffek *et al.*, "Understanding the quenching effects of aromatic C-H- and C-D-oscillators in near-IR lanthanoid luminescence," *J. Am. Chem. Soc.*, vol. 134, no. 39, pp. 16413–16423, 2012.

[22] M. P. Tsvirko, S. B. Meshkova, V. Y. Venchikov, Z. M. Topilova, and D. V Bol'shoi, "Determination of contributions of various molecular groups to nonradiative deactivation of electronic excitation energy in β-diketonate complexes of ytterbium(III)," *Opt. Spectrosc.*, vol. 90, no. 5, pp. 669–673, 2001.

[23] H. W. Leverenz, *An Introduction to Luminiscence of Solids*. Dover Publications, 1968.

[24] B. Zhou, B. Shi, D. Jin, and X. Liu, "Controlling upconversion nanocrystals for emerging applications," *Nat. Nanotechnol.*, vol. 10, no. 11, pp. 924–936, 2015.

[25] F. Auzel, "Upconversion and Anti-Stokes Processes with f and d Ions in Solids," *Chemical Reviews*, vol. 104, no. 1. pp. 139–173, 2004.

[26] H. Dong, L. D. Sun, and C. H. Yan, "Energy transfer in lanthanide upconversion

studies for extended optical applications," *Chem Soc Rev*, vol. 44, no. 6, pp. 1608–1634, 2015.

[27] L. Aboshyan-Sorgho *et al.*, "Near-infrared→Visible light upconversion in a molecular trinuclear d-f-d complex," *Angew. Chemie - Int. Ed.*, vol. 50, no. 18, pp. 4108–4112, 2011.

[28] A. Nonat *et al.*, "Room temperature molecular up conversion in solution," *Nat. Commun.*, vol. 7, no. May, p. 11978, 2016.

[29] I. Hernández, N. Pathumakanthar, P. B. Wyatt, and W. P. Gillin, "Cooperative infrared to visible up conversion in Tb3+, Eu 3+, and Yb3+ containing polymers," *Adv. Mater.*, vol. 22, no. 47, pp. 5356–5360, 2010.

[30] L. de S. Menezes, G. S. Maciel, C. B. De Araújo, and Y. Messaddeq, "Phonon-assisted cooperative energy transfer and frequency upconversion in a Yb3+/Tb3+ codoped fluoroindate glass," *J. Appl. Phys.*, vol. 94, no. 2, pp. 863–866, 2003.

[31] W. Strek, P. Deren, and A. Bednarkiewicz, "Cooperative processes in KYb (WO) crystal doped with Eu and Tb ions," *J. Lumin.*, vol. 89, pp. 999–1001, 2000.

[32] M. Pollnau, D. R. Gamelin, S. R. Lüthi, H. U. Güdel, and M. P. Hehlen, "Power dependence of upconversion luminescence in lanthanide and transition-metal-ion systems," *Phys. Rev. B*, vol. 61, no. 5, pp. 3337–3346, 2000.

[33] W. Strek, P. Deren, and A. Bednarkiewicz, "Cooperative processes in KYb (WO) crystal doped with Eu and Tb ions," *J. Lumin.*, vol. 89, pp. 999–1001, 2000.

[34] M. Pollnau, D. R. Gamelin, S. R. Lüthi, H. U. Güdel, and M. P. Hehlen, "Power dependence of upconversion luminescence in lanthanide and transition-metal-ion systems," *Phys. Rev. B*, vol. 61, no. 5, pp. 3337–3346, 2000.

[35] J. H. Chung, J. H. Ryu, S. Y. Lee, S. H. Kang, and K. B. Shim, “Effect of Yb3+ and Tm3+ concentrations on blue and NIR upconversion luminescence in Yb3+, Tm3+ co-doped CaMoO4,” *Ceram. Int.*, vol. 39, no. 2, pp. 1951–1956, 2013.

[36] M. V. D. Vermelho *et al.*, “Thermally enhanced cooperative energy-transfer frequency upconversion in terbium and ytterbium doped tellurite glass,” *J. Lumin.*, vol. 102–103, no. SPEC, pp. 762–767, 2003.

[37] G. Mancino, A. J. Ferguson, A. Beeby, N. J. Long, and T. S. Jones, “Dramatic increases in the lifetime of the Er3+ ion in a molecular complex using a perfluorinated imidodiphosphinate sensitizing ligand,” *J. Am. Chem. Soc.*, vol. 127, no. 2, pp. 524–525, 2005.

[38] H.-Q. Ye *et al.*, “Effect of Fluorination on the Radiative Properties of Er3+ Organic Complexes: An Opto-Structural Correlation Study,” *J. Phys. Chem. C*, vol. 117, no. 45, pp. 23970–23975, 2013.

[39] N. M. Shavaleev, R. Scopelliti, F. Gumy, and J. C. G. Bünzli, “Surprisingly bright near-infrared luminescence and short radiative lifetimes of ytterbium in hetero-binuclear Yb-Na chelates,” *Inorg. Chem.*, vol. 48, no. 16, pp. 7937–7946, 2009.

[40] B. S. Cao, Y. Y. He, L. Zhang, and B. Dong, “Upconversion properties of Er3+-Yb3+:NaYF4 phosphors with a wide range of Yb3+ concentration,” *J. Lumin.*, vol. 135, no. 18, pp. 128–132, 2013.

[41] D. Xu, C. Liu, J. Yan, S. Yang, and Y. Zhang, “Understanding energy transfer mechanisms for tunable emission of Yb3+-Er3+ Codoped GdF3 nanoparticles: Concentration-dependent luminescence by near-infrared and violet excitation,” *J. Phys. Chem. C*, vol. 119, no. 12, pp. 6852–6860, 2015.

[42] H. Lu, W. P. Gillin, and I. Hernández, “Concentration dependence of the up- and

down-conversion emission colours of Er(3+)-doped Y2O3: a time-resolved spectroscopy analysis.," *Phys. Chem. Chem. Phys.*, vol. 16, no. 38, pp. 20957–63, 2014.

[43] V. D. Bock, H. Hiemstra, and J. H. Van Maarseveen, "Cu I-catalyzed alkyne-azide 'click' cycloadditions from a mechanistic and synthetic perspective," *European J. Org. Chem.*, no. 1, pp. 51–68, 2006.

[44] Y. G. Gololobov and L. F. Kasukhin, "Recent advances in the staudinger reaction," *Tetrahedron*, vol. 48, no. 8, pp. 1353–1406, 1992.

[45] I. Szele and H. Zollinger, *Azo coupling reactions structures and mechanisms*, vol. 112. 1983.